JOURNAL OF UNDERGRADUATE RESEARCH

TRIP13 is Critical for the Survival of B-cell Lymphomas and Myeloid Leukemias in Vitro

Gene Pozas, Julian Tobon, Reem Abdelghany, Jacob Fingeret, Emma Noel, Vedant Ramachandran, Jana Opavska, Rene Opavsky

College of Liberal Arts and Sciences, University of Florida

Rene Opavsky PhD, Department of Anatomy and Cell Biology

Abstract

Hematologic malignancies represent a diverse group of blood tumors accounting for approximately 10% of all cancer cases in the US. Based on the site of manifestation, presumed cell of origin, genetic abnormalities, and clinical features, we recognize more than 100 clinically important subtypes of hematologic malignancies broadly categorized into three main groups: leukemia, lymphoma, and multiple myeloma. While the prognosis for patients with specific subtypes of hematologic malignancies, such as Hodgkin lymphomas or chronic lymphocytic leukemia has significantly improved over the last several years, other subtypes such as acute myeloid leukemia or non-Hodgkin lymphomas still present with significant treatment challenges. A better understanding of molecular drivers of tumor maintenance is needed to improve existing therapies. Thyroid hormone receptor interactor 13 (TRIP13) is an AAA + ATPase that plays an important yet poorly understood role in the regulation of the mammalian cell cycle. The *TRIP13* gene is highly expressed in various human tumors including colorectal carcinoma and glioblastoma, and it seems to promote tumorigenesis. Recently, we identified *TRIP13* as a gene overexpressed in Peripheral T-cell lymphomas where it plays a critical role in tumor maintenance by regulating the G2-M phase of the cell cycle. However, the biological activities of TRIP13 in non-T cell hematologic malignancies have not been investigated to date. Here we used shRNA-mediated knockdown and a small molecule inhibitor to downregulate *TRIP13* in B-cell lymphoid and myeloid lineages. We found genetic downregulation inhibited the proliferation of both B-cell lymphomas and acute myeloid leukemia cell lines *in vitro*. The pharmacologic inhibition of TRIP13 effectively induced the G0/G1 cell cycle arrest and apoptosis of B-cell lymphomas. Altogether these data demonstrate that TRIP13 is critical for the maintenance of hematologic malignancies of B-cell and myeloid malignancies *in vitro*. Thus, TRIP13 might be a good target in the treatment of various types of hematologic malignancies.

Keywords: TRIP13, Hematologic Malignancies, Lymphoma, Myeloma, Tumor Maintenance

Introduction

Hematological malignancies are myeloid and lymphoid tumors caused by disruption of normal functions in blood cells. Based on various cellular and molecular features, they are divided into several common subtypes, consisting of leukemia, multiple myeloma (MM), non-Hodgkin lymphoma (NHL), and Hodgkin lymphoma (HL) (Demlaj, 2019). The incidence of

hematologic malignancies varies based on subtype, age, gender, geography, and demographics. It is estimated that almost 185,000 people in the US were diagnosed with leukemia, lymphoma, or myeloma in 2023 (The Leukemia & Lymphoma Society, 2023). The treatment options for patients include radiation therapy, chemotherapy, bone marrow transplantation, chimeric antigen receptor (CAR) T-cell therapy, and others. While the survival rates for many hematologic malignancies have risen in recent years, the prognosis for patients with subtypes of leukemia and lymphoma remains unsatisfactory. For example, the overall 5-year relative survival rate for acute myeloid leukemia (AML) is approximately 30% (SEER*Explorer, 2024). Despite tremendous progress in understanding the molecular basis of hematologic malignancies, our understanding of disease drivers remains inadequate. To improve treatments, the identification of genes critical for the survival of leukemia and lymphoma cells is clearly needed.

TRIP13 (thyroid hormone receptor interactor 13) is the AAA+ ATPase that contributes to the regulation of the cell cycle by controlling the mitotic spindle assembly checkpoint, meiotic recombination, and DNA repair (Jeong, 2022). The decrease in TRIP13 inhibits the proliferation and metastatic potential of colorectal carcinoma cells, as well as other cancer cell types including Non-Small Cell Lung Cancer (NSCLC) and ovarian cancer, demonstrating the broad impact of TRIP13 inhibition on various malignancies. (Agarwal, 2022 & 2020; Liu, 2019; Xu, 2020). Recent studies have highlighted the potential of TRIP13 as a therapeutic target, demonstrating that its inhibition can synergize with Aurora kinase inhibitors to induce apoptosis in HPV-positive cancers, and with PARP1 inhibitors to enhance DNA damage and cell death in hepatocellular carcinoma (Ghosh, 2022; Xu, 2022). We recently found that TRIP13 is critical for the proliferation and survival of T-cell lymphomas (Nowialis, 2024). Here we asked whether TRIP13 is required for the proliferation of B-cell and myeloid malignancies.

Methods

Plasmid DNA Constructs

To facilitate gene knockdown studies, we utilized lentiviral vectors designed to express short hairpin RNAs (shRNAs), chosen for their efficiency in delivering genetic material into both dividing and non-dividing cells, making them ideal for stable gene knockdown in various cell types. We obtained two specific lentiviral constructs from Vector Builder: pLV[shRNA]-

mCherry-U6>Scrambled[shRNA#1] with a target sequence of CCTAAGGTTAAGTCGCCCTCG and pLV[shRNA]-mCherry-U6>hTRIP13[shRNA#1] with a target sequence of GCTACTCAACAGACATAATAT. The scrambled construct serves as a control, expressing a non-targeting shRNA to account for any non-specific effects of shRNA expression and viral transduction. The TRIP13 construct targets the human *TRIP13* gene, which is of particular interest due to its role in cancer cell proliferation and maintenance, specifically in Peripheral T-Cell Lymphoma (PTCL). By knocking down *TRIP13*, we aim to investigate its specific functions and the resulting phenotypic effects on cancer cells. Both constructs include an mCherry reporter gene under the control of the U6 promoter, enabling easy visualization and confirmation of successful transduction. The choice of these constructs and the specific shRNA sequences was informed by previous literature indicating their efficacy in knocking down their respective targets. Additionally, the use of lentiviral vectors ensures stable integration of the shRNA expression cassette into the host genome, providing long-term gene knockdown and consistent experimental results.

Cell Lines and Lentiviral Production

Human Raji (Burkitt's B-cell lymphoma; CCL-86) and K562 (chronic myelogenous leukemia; CCL-243) cell lines were obtained from the American Type Culture Collection (ATCC), while the Lenti-XTM 293T cell line was purchased from Takara (#632180). These cell lines were periodically checked for karyotype integrity and tested for mycoplasma contamination, ensuring the reliability of experimental results. Only early passages were used to maintain cell line integrity. The cells were maintained in either DMEM or RPMI 1640 media (Invitrogen) supplemented with 10% fetal bovine serum, and cultured at 37°C in a humidified atmosphere with 5% CO2. The cells were passaged according to standard recommendations to ensure optimal growth conditions. For lentivirus production, 293T cells were seeded in 100 mm tissue culture plates to achieve approximately 80-90% confluence before transfection. The cells were then transfected with a mixture of plasmid DNA, and packaging plasmids psPAX2 and pMD2.G, at a ratio of 1:0.65:0.35, using 70 µg of polyethylenimine (PEI) (Polysciences) as the transfection reagent. Lentiviral particles were harvested 48-96 hours post-transfection. For transduction, cells were infected as previously described by Hlady (2011), utilizing Polybrene

Infection/Transfection Reagent (Sigma) to enhance infection efficiency. The transduction efficiency was assessed by measuring the percentage of mCherry-positive cells using fluorescence-activated cell sorting (FACS).

FACS, BrdU Incorporation, and Apoptosis Assays

For shRNA experiments, the growth of Raji or K562 cells transduced with lentiviruses was monitored by FACS over a period of 3 to 11 days. The maximum percentage of mCherry-expressing cells was typically observed 72 hours post-transduction. Subsequent mCherry data points were normalized to this time point and expressed as a relative percentage of the initial measurement. Periodic measurements of mCherry expression were conducted using flow cytometry on the LSRII available at the University of Florida flow cytometry core facility. Cell growth was evaluated by Trypan blue staining and cell counting at various time points to assess proliferation and viability. Additionally, cell viability was evaluated by scoring the percentage of cells in the "live gate" of FACS diagrams obtained at different time points. For *in vitro* labeling, BrdU at a concentration of 0.01 mM was added 110 minutes before cell harvest. BrdU-positive cells were quantified using anti-BrdU-FITC from the BrdU Flow Kit (BD Biosciences Pharmingen), following the manufacturer's instructions. Cell cycle analysis involved the addition of 7-aminoactinomycin D (7-AAD) to the samples, while apoptosis was assessed by staining cells with allophycocyanin-conjugated annexin V antibody and analyzing them by FACS according to the manufacturer's recommendations (eBioscience). FACS analysis was performed using the BD Accuri C6 Plus Flow Cytometer and data analysis was conducted using FlowJo X software.

TRIP13 Drug Treatment, Cell Counting, and Molecular Assays.

For TRIP13 drug treatment, cell counting, and molecular assays, DCZ0415, an inhibitor of TRIP13, was obtained from MedChem (Cat. #: HY-130603) and dissolved in DMSO. Raji cells were treated with either DMSO (serving as the vehicle control) or DCZ0415 at concentrations ranging from 1 to 25 μM per 1 mL of culture medium. Cell viability was assessed at various time points following drug addition using Trypan Blue exclusion dye and cell counting. The Trypan Blue exclusion method allows for the differentiation between viable and

non-viable cells based on membrane integrity. In addition to cell viability assays, BrdU incorporation assays were performed to evaluate cell proliferation, and apoptosis assays were conducted as described above. For BrdU assays, cells were labeled with BrdU and then quantified using anti-BrdU-FITC, following the manufacturer's protocol. Apoptosis was assessed by staining cells with allophycocyanin-conjugated annexin V antibody and analyzing them via flow cytometry. These assays provided comprehensive data on the effects of TRIP13 inhibition on cell growth, proliferation, and survival.

Statistical Analysis

The statistical significance of means ±SEM was evaluated using the two-tailed Student's t-test. For all statistical analyses p values < 0.05 were considered significant.

Results

TRIP13 is overexpressed in B-cell Lymphomas and Myeloid Leukemias

We previously reported that the *TRIP13* gene is overexpressed in primary T-cell malignancies (Nowialis, 2024). To determine if *TRIP13* overexpression occurs in other types of hematologic malignancies, we performed an analysis of the datasets in the HEMAP database (Pölönen, 2019). This analysis revealed that *TRIP13* is significantly up-regulated not only in T-cell malignancies (TCL and T-ALL) but also in a majority of AML, B-Cell Lyphoma (BCL), Pre-B cell leukemia, B-lymphoid, and multiple myelomas (Figure 1A, B). In contrast, levels of *TRIP13* were mostly unchanged in Chronic Lymphocytic Leukemia (CLL) and a subset of myeloid malignancies (Figure 1A, B). Thus, a majority of aggressive hematologic malignancies express elevated levels of *TRIP13*, highlighting the possibility that cancer cells may require this protein for their proliferation.

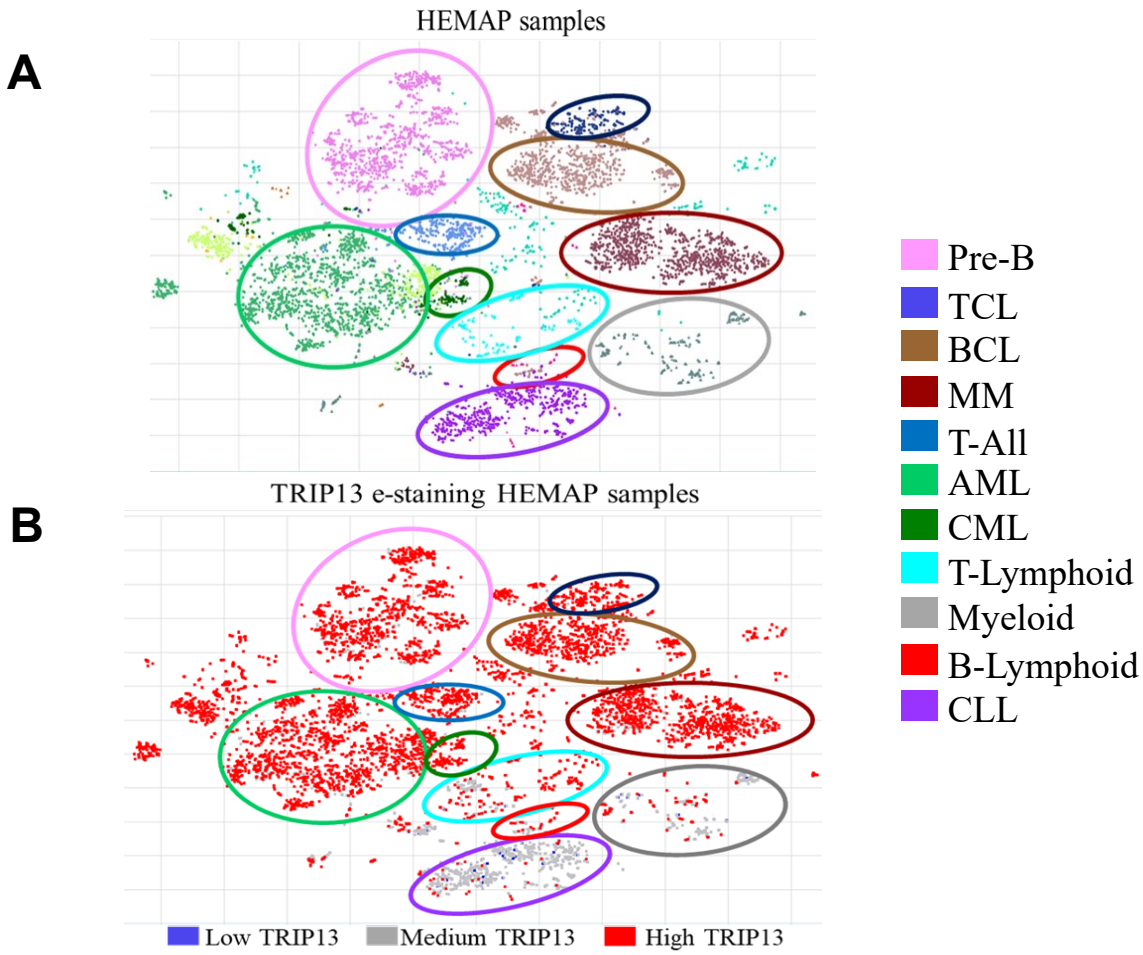

Figure 1. *TRIP13* is overexpressed in B-cell lymphomas and myeloid leukemias.

(A) The transcriptome data projected in 2D by t-SNE in the indicated cancer types, cell lines, and normal cell populations with each dot representing one sample (HEMAP). The separation between annotated disease types (indicated by color) is shown for distinct clusters visible on the cancer map. **(B)** Visualization of *TRIP13* expression on a t-SNE map, with red, grey, and blue dots corresponding to high, medium, and low scores of *TRIP13* expression, respectively.

TRIP13 Downregulation Inhibits the Proliferation of Malignant Myeloid Leukemia and B-cell Lymphoma Cell Lines

Our previous data demonstrated that TRIP13 has a critical role in the maintenance of PTCL cell lines in vitro (Nowialis, 2024) but its role in other types of hematologic malignancies remains unclear. To determine if TRIP13 is required for the proliferation of myeloid and B-cell lines, we transduced K562 (myeloid leukemia) and Raji (B-cell lymphoma) cell lines with lentiviruses expressing shRNAs either targeting *scrambled* or *TRIP13* and co-expressing mCherry. We previously used these constructs and demonstrated that while the expression of *scrambled* shRNA had no effects, *TRIP13* shRNA strongly downregulated the TRIP13 protein (Nowialis, 2024). Cells were continuously cultured over 11 days, and the percentage of mCherry-positive cells was measured at various time points by FACS. In our settings, the expression of the fluorescent protein mCherry allows us to identify cells that were transduced with lentiviruses (co-expressing shRNA and mCherry) and evaluate the behavior of transduced cells on a background of non-transduced cells that serve as controls for the baseline cellular proliferation of the particular cell line. The percentage of cells expressing *scrambled* shRNA remained relatively stable, suggesting that the expression of *scrambled* shRNA or mCherry did not affect the proliferation of cells (Figures 2A-D). In contrast, the percentage of *TRIP13* shRNA-1 expressing cells was gradually reduced over time, suggesting that the proliferation of K562 and Raji cells is impaired by *TRIP13* downregulation (Figures 2A-D). The proliferative defect was reproducible and was also seen using independent *TRIP13* shRNA-2 (data not shown). K562 and Raji cells transduced with lentiviruses expressing shRNA against *scrambled* or *TRIP13*. At days 3 and 11 of continuous culturing, *TRIP13* shRNA showed a significant reduction in mCherry-positive cells compared to *scrambled* shRNA. mCherry expression at day 3 was normalized to 100% for *scrambled* shRNA, and the percentage of mCherry-positive cells for *TRIP13* shRNA was plotted relative to *scrambled* shRNA at each time point. Altogether, these data suggest that the downregulation of *TRIP13* has antiproliferative effects on K562 and Raji cell lines raising a possibility that this protein is critical for the survival of myeloid and B-cell malignancies. Thus, its targeting may be beneficial in the treatment of these malignancies.

.

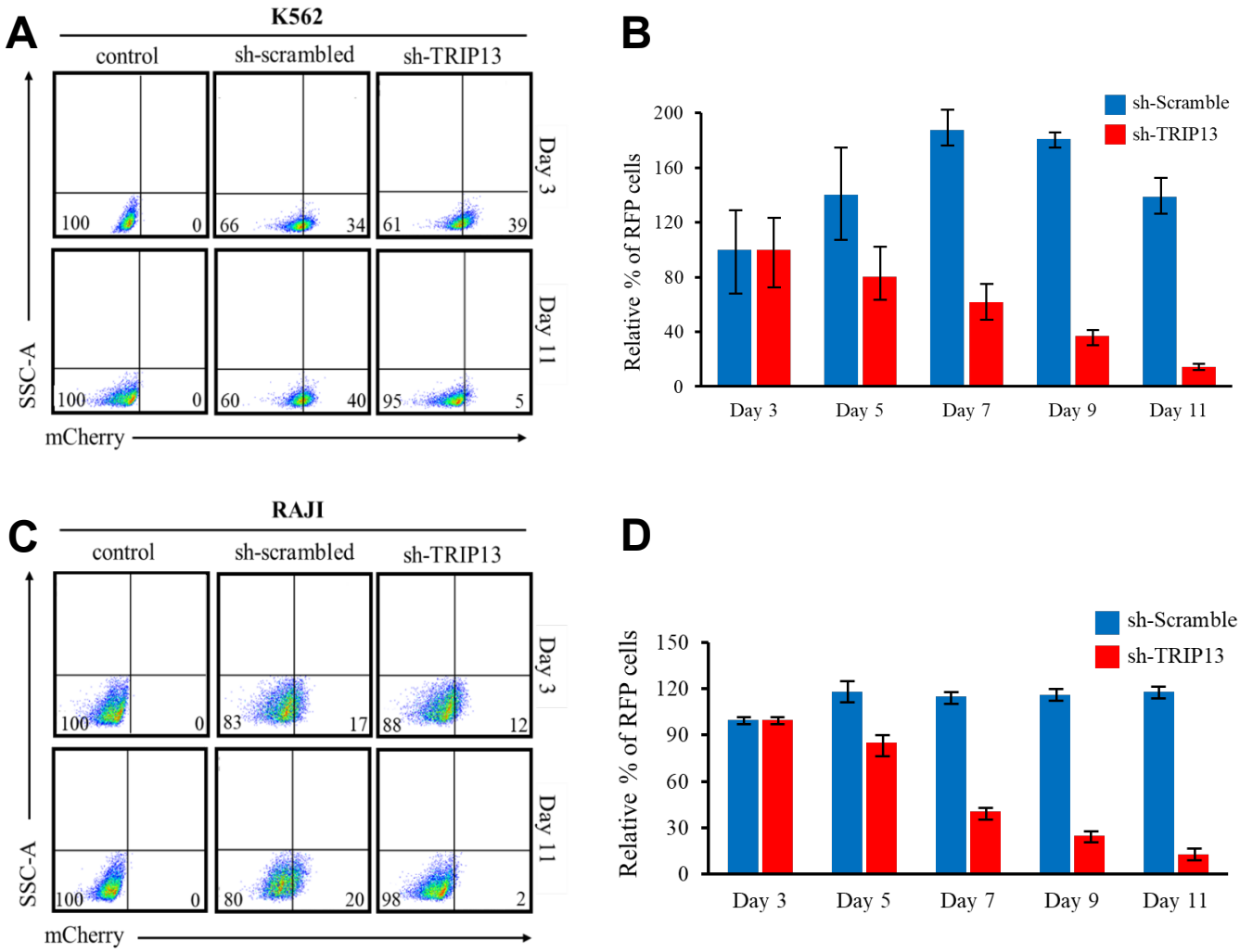

Figure 2. *TRIP13* downregulation results in impaired cellular proliferation of malignant myeloid and B-lymphoid cells.

(A) Representative FACS diagrams showing mCherry (RFP) expression in K562 cells transduced with lentiviruses expressing *scrambled* or *TRIP13* shRNA at days 3 and 11. Numbers indicate percentages from quadrant statistics using FlowJo X software. **(B)** Relative mCherry (RFP) expression in K562 cells transduced with *scrambled* or *TRIP13* shRNA, measured by FACS at day 3 and up to day 11. Transduction efficiency on day 3 was normalized to 100% for *scrambled*. Values for *TRIP13* shRNA are plotted relative to *scrambled*. Data are presented as mean ±SEM (from three independent experiments) relative to scrambled, *$p < 0.05$. p values were calculated by a two-tailed Student's t-test. **(C)** Representative FACS diagrams showing mCherry expression in Raji cells transduced with lentiviruses expressing *scrambled* or *TRIP13* shRNA at days 3 and 11. Numbers indicate percentages from quadrant statistics using FlowJo X software. **(D)** Relative mCherry (RFP) expression in Raji cells transduced with *scrambled* or *TRIP13* shRNA, measured by FACS at day 3 and up to day 11. Transduction efficiency on day 3 was normalized to 100% for *scrambled*. Values for *TRIP13* shRNA are plotted relative to *scrambled*. Data are presented as mean ±SEM (from three independent experiments) relative to *scrambled*, *$p < 0.05$. p values were calculated by a two-tailed Student's t-test.

Treatment with TRIP13 Inhibitor DCZ0415 Inhibits the Proliferation of B-cell Lymphoma Raji Cells

To test if targeting TRIP13 may have therapeutic potential in B-cell lymphomas, we next treated the Raji lymphoma cell line with DCZ0415, a TRIP13-specific inhibitor (Agarwal, 2022). The treatment of Raji cells with vehicle DMSO had no impact on the viability of the cell culture as measured by the percentage of cells in the "live gate" of the forward/scatter diagram of FACS analysis. In contrast, the treatment of Raji cells with a 10 μM concentration of DCZ0415 resulted in a severe reduction in cellular viability from ~90% to 77% on day 2 and to 58% on day 4 of the treatment (Figure 3A). The treatment of the same cell line with a 20 μM concentration had a more pronounced cell-killing effect, reducing cellular viability to 71% on day 2 and 40% on day 4 (Figure 3A). For the 10 μM concentration of DCZ0415, this corresponds to a decrease in relative viability on days 2 and 4 by 15% and 40%, respectively. The 20 μM concentration of DCZ0415 caused a 60% decrease in relative viability on day 4 (Figure 3B). Thus, the pharmacological inhibition of TRIP13 using DCZ0415 results in the death of B-cell lymphoma cells, formally demonstrating that inhibition of TRIP13 has therapeutic potential for the treatment of hematologic malignancies of B-cell and myeloid origin.

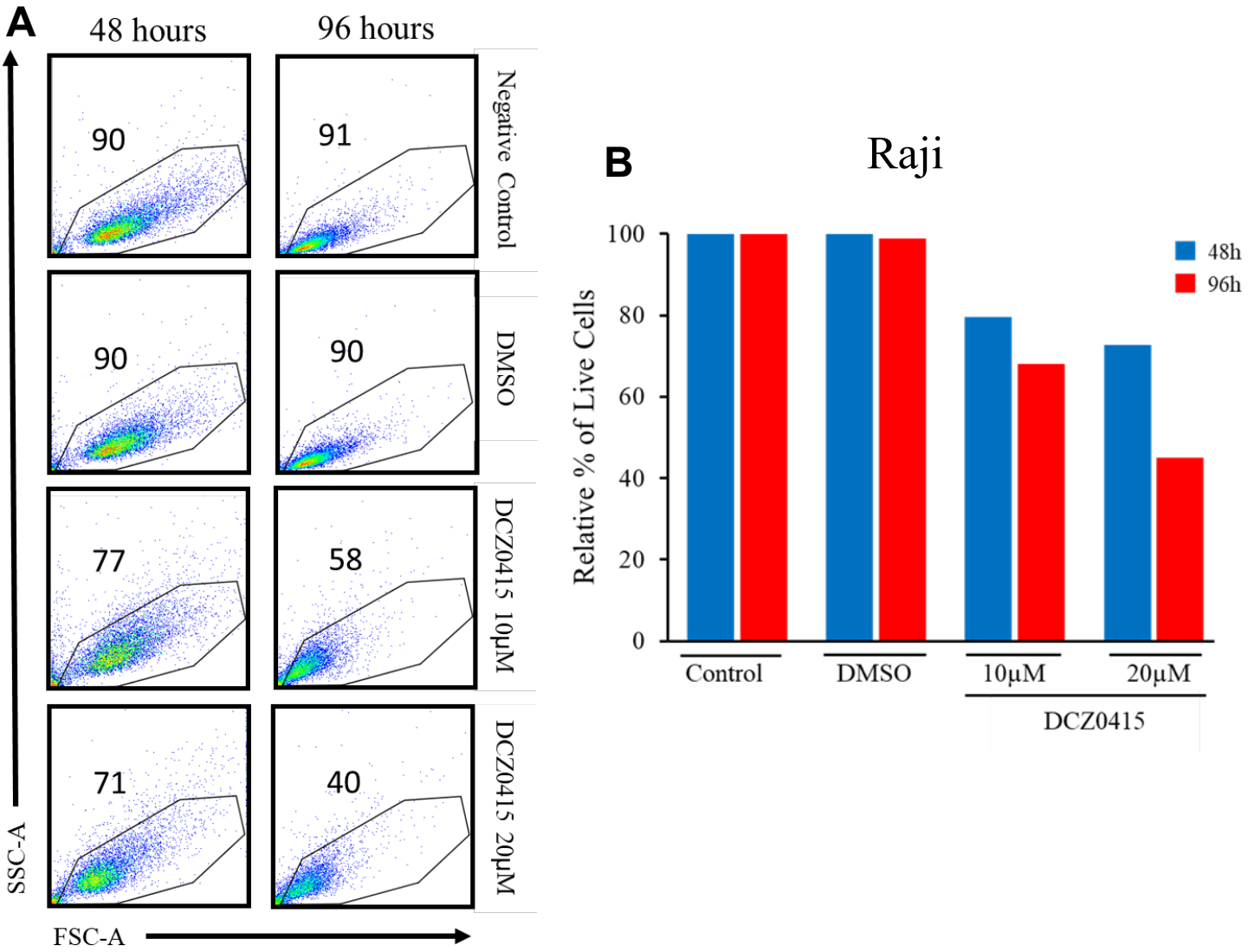

Figure 3. Pharmacological TRIP13 inhibition by DCZ0415 results in impaired cellular proliferation of Raji cells.

(A) Representative examples of FACS diagrams indicating the percentage of Raji cells in the "live gate" at 48 hours and 96 hours after treatment with either DMSO (vehicle) or DCZ0415 at indicated concentrations. Untreated control cells are also shown. **(B)** The relative percentage of live untreated control Raji cells and cells treated with either DMSO, 10μM DCZ0415 or 20μM DCZ0415 as measured by FACS analysis. Viability was determined as the percentage of cells in the "live gate" in forward scatter FACS diagrams at 48 hours and 96 hours after treatment. The values obtained for the percentage of live cells at each time point were plotted relative to the percentage in untreated control cells.

DCZ0415 Treatment of Raji Cells Induces G0/G1 Arrest and Cell Death.

To uncover which phases of the cell cycle are affected, we next measured the ability of Raji cells to incorporate BrdU (S phase) upon the treatment with TRIP13 inhibitor. Approximately 55% of control Raji cells that were not treated with DCZ0415 incorporated BrdU during a 90-minute BrdU pulse *in vitro* at a time point of 48 hours (Figure 4A). Similarly, ~45% of Raji cells treated with a DMSO vehicle incorporated BrdU at a 2-day time point (Figure 4A). The treatment of Raji cells with 10 μM DCZ0415 resulted in several cells capable of incorporating BrdU after 48 hours and even more after 96 hours of treatment with the drug (27% and 11% respectively) (Figure 4A). The treatment of Raji cells with 20 μM DCZ0415 ablated the ability of almost all cells to incorporate BrdU at both time points (less than 1%) (Figure 4A). These data suggest that the inhibition of TRIP13 activity by DCZ0415 severely impaired the ability of B-cell lymphoma cells to enter the S phase of the cell cycle.

To gain a broader insight into cell cycle defects, we also stained cells with DNA intercalating agent 7-Aminoactinomycin D (7-AAD). FACS analysis of DNA content revealed that the drug treatment induced G0/G1 arrest with an increasing amount of sub-G0 DNA content events (dead cells) over time cells (Figures 4B**, C**). Consistently with observed cell death, the treatment with DCZ0415 resulted in increased levels of apoptotic marker, Annexin V, suggesting that G0/G1 arrest is followed by apoptosis (Figure 4D).

Altogether, our data show that TRIP13 inhibition resulted in decreased BrdU incorporation, G0/G1 arrest, increased Annexin V expression, and apoptosis.

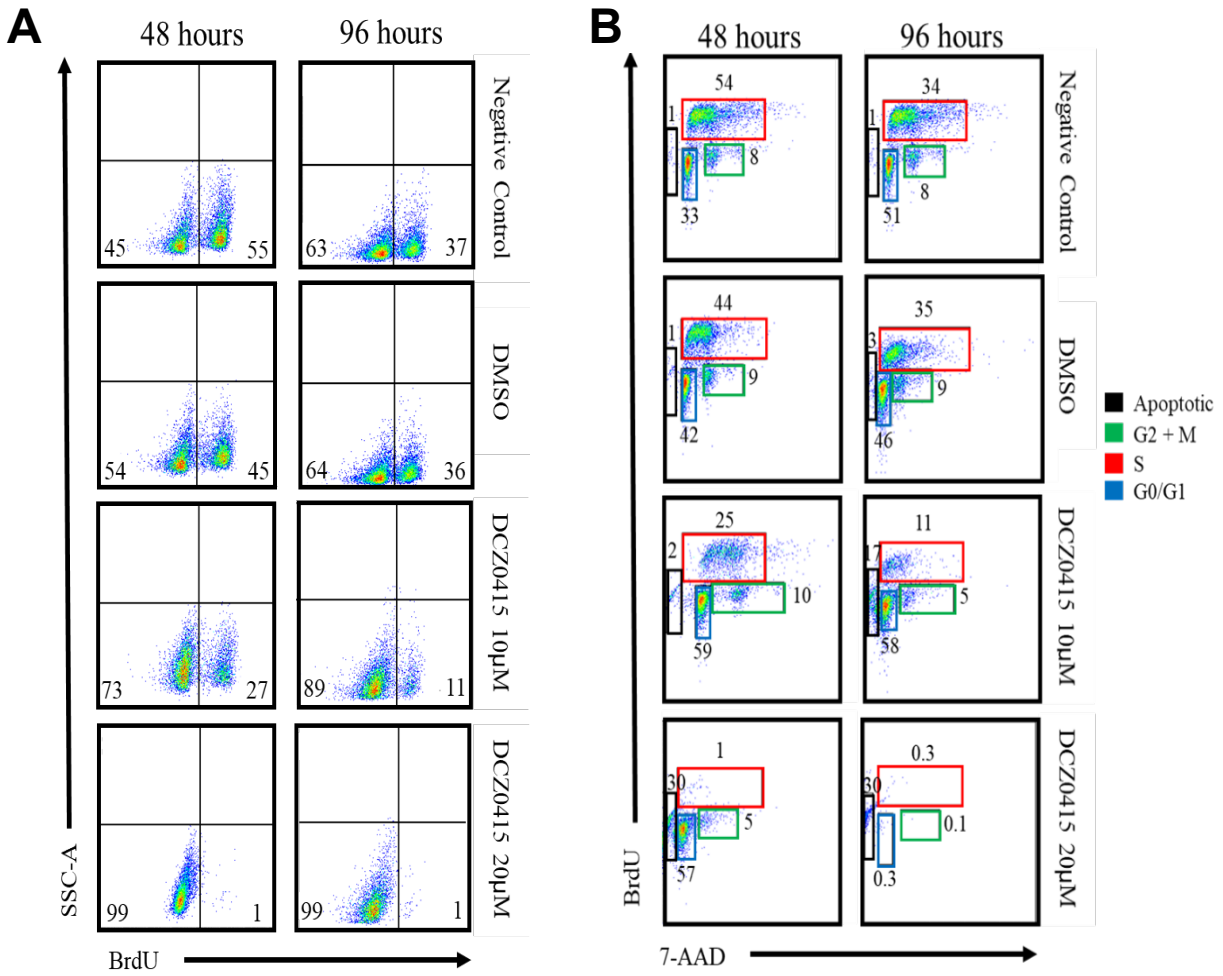
A
48 hours
96 hours
Negative Control
DMSO
DCZ0415 10μM
DCZ0415 20μM
45
55
63
37
54
45
64
36
73
27
89
11
99
1
99
1
SSC-A
BrdU
B
48 hours
96 hours
54
1
8
33
34
1
8
51
44
1
9
42
35
3
9
46
25
2
10
59
11
17
5
58
1
30
5
57
0.3
30
0.1
0.3
BrdU
7-AAD
Apoptotic
G2 + M
S
G0/G1

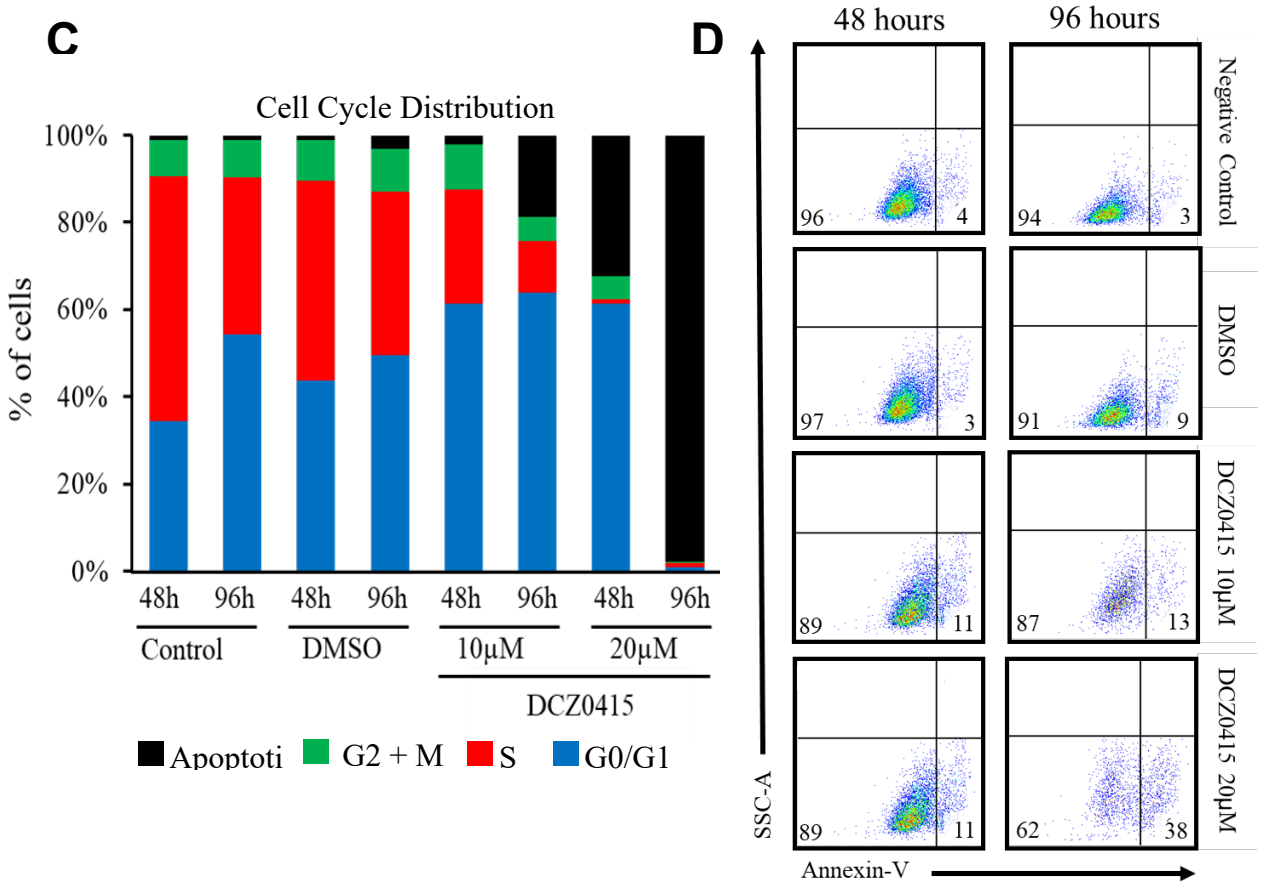

Figure 4. Pharmacological TRIP13 inhibition by DCZ0415 inhibits cellular growth by inducing G0/G1 arrest and cell death of Raji cells.

(A) Representative FACS diagrams of the BrdU incorporation assay of Raji cells treated with either DMSO, 10μM DCZ0415 or 20μM DCZ0415 after 48 and 96 hours. Untreated control cells are also shown. Numbers in corners of FACS diagrams represent percentages obtained from quadrant statistics using FlowJo X software. **(B)** Representative FACS diagrams obtained from cell cycle analysis of Raji cells treated with either DMSO, 10μM DCZ0415, or 20μM DCZ0415 after 48 and 96 hours. Untreated control cells are also shown. A combination of BrdU incorporation assay and staining with 7-ADD followed by FACS was used. **(C)** Cell cycle distribution of Raji cells. Percentage of cells in various phases of the cell cycle in Raji cells treated with either DMSO, 10μM DCZ0415 or 20μM DCZ0415 after 48 and 96 hours. Untreated control cells are also shown. The numbers used to generate stacked graphs were obtained by analysis shown in **B** using the FACS data obtained from BrdU incorporation assay coupled with 7-AAD staining and analyzed by FlowJo X software. **(D)** Representative FACS diagrams obtained from Annexin V assays of Raji cells treated with either DMSO, 10μM DCZ0415 or 20μM DCZ0415 after 48 and 96 hours. Untreated control cells are also shown. The percentage of Annexin V positive cells in the FACS profile is shown within the bottom right corner of each plot and indicates ongoing apoptosis.

Discussion

We previously demonstrated that both genetic downregulation and pharmacological inhibition of TRIP13 in human T-cell leukemia and lymphoma cell lines were associated with the G2-M arrest of the cell cycle and cell death. Unexpectedly, here we found that TRIP13 inhibitor induced the G0/G1 arrest of the cell cycle suggesting that different molecular and cellular mechanisms may be involved in response to TRIP13 inhibition in B-cells. One key difference between the T-cell lines used in the previous study (Nowialis, 2024) and the Raji B-cell line used here is the fact that this cell line is derived from Burkitt's lymphoma patient. A vast majority of Burkitt's lymphomas have genomic translocations that activate the expression of c-MYC proto-oncogene. C-MYC is known to be critical for the G1-S transition of the cell cycle. A previous report suggested that TRIP13 can inhibit a negative regulator of c-MYC levels - an E3 ubiquitin ligase FBXW7 (Zhang, 2019). Thus, the downregulation of TRIP13 may up-regulate FBXW7 which in turn could result in c-MYC downregulation in the Raji cell line resulting in growth arrest in the G0/G1 phase of the cell cycle. The effects of c-MYC down-regulation might be more pronounced in Burkitt's lymphoma cell line than T-cell lines due to "oncogene addiction" of the Raji cell line to high levels of c-MYC. While the precise details of the mechanism by which the decrease in TRIP13 levels causes the G0/G1 cell cycle arrest in Raji have yet to be worked out, it is clear that targeting TRIP13 results in the death of B-cell lymphoma and chronic myelogenous leukemia cells. Our data thus expands the repertoire of malignancies whose cell survival is dependent on TRIP13. Thus, TRIP13 inhibition may be helpful in the future treatment of a variety of hematologic malignancies.

Acknowledgments

The authors would like to express their sincere gratitude to their principal investigator for his guidance and support throughout the research project. They are also immensely thankful to their lab manager, graduate student mentor, and the rest of the lab for their assistance and contributions to this paper.

References

Agarwal S, Behring M, Kim HG, Chandrashekar DS, Chakravarthi BVSK, Gupta N, Bajpai P, Elkholy A, Al Diffalha S, Datta PK, Heslin MJ, Varambally S, Manne U. TRIP13 promotes metastasis of colorectal cancer regardless of p53 and microsatellite instability status. Mol Oncol. 2020 Dec;14(12):3007-3029. doi: 10.1002/1878-0261.12821. Epub 2020 Oct 28. PMID: 33037736; PMCID: PMC7718953.

Agarwal, S., et al. (2022). DCZ0415, a small-molecule inhibitor targeting TRIP13, inhibits EMT and metastasis via inactivation of the FGFR4/STAT3 axis and the Wnt/β-catenin pathway in colorectal cancer. *Molecular Oncology, 16*(10), 1728-1745. https://doi.org/10.1002/1878-0261.13201

Damlaj, M., El Fakih, R., & Hashmi, S. K. (2019). Evolution of survivorship in lymphoma, myeloma and leukemia: Metamorphosis of the field into long-term follow-up care. *Blood Reviews, 33*, 63-73. https://doi.org/10.1016/j.blre.2018.07.003

Ghosh, S., Mazumdar, T., Xu, W., Powell, R. T., Stephan, C., Shen, L., Shah, P. A., Pickering, C. R., Myers, J. N., Wang, J., Frederick, M. J., & Johnson, F. M. (2022). Combined TRIP13 and Aurora Kinase Inhibition Induces Apoptosis in Human Papillomavirus–Driven Cancers. *Clinical Cancer Research, 28*(20), 4479-4493. https://doi.org/10.1158/1078-0432.CCR-22-1627

Hlady, R. A., et al. (2011). Loss of Dnmt3b function upregulates the tumor modifier Ment and accelerates mouse lymphomagenesis. *Journal of Clinical Investigation, 122*(1), 163-177. https://doi.org/10.1172/JCI57292

Jeong, H., et al. (2022). TRIP13 Participates in Immediate-Early Sensing of DNA Strand Breaks and ATM Signaling Amplification through MRE11. *Cells, 11*(24). https://doi.org/10.3390/cells11244095

Liu, J., et al. (2019). TRIP13 is a prognostic biomarker and promotes cell proliferation and invasion in non-small cell lung cancer. *BMC Cancer, 19*(1), 464. https://doi.org/10.1186/s12885-019-5688-5

Nowialis, P., Tobon, J., Lopusna, K., Opavska, J., Badar, A., Chen, D., Abdelghany, R., Pozas, G., Fingeret, J., Noel, E., Riva, A., Fujiwara, H., & Opavsky, R. (2024). Genome-wide methylation profiling of Peripheral T-cell lymphomas identifies TRIP13 as a critical driver of tumor proliferation and survival. *Research Square [Preprint]*. https://doi.org/10.21203/rs.3.rs-3971059/v1. PMID: 38464090; PMCID: PMC10925438. https://www.ncbi.nlm.nih.gov/pmc/articles/PMC10925438/

Pölönen, P., Mehtonen, J., Lin, J., Liuksiala, T., Häyrynen, S., & Teppo, S. (2019). Hemap: an Interactive Online Resource for Characterizing Molecular Phenotypes across Hematologic Malignancies. *Cancer Research, 79*(10), 2466-2479.

SEER*Explorer: An interactive website for SEER cancer statistics [Internet]. Surveillance Research Program, National Cancer Institute; 2023 Apr 19. [updated: 2023 Nov 16; cited 2024 Mar 30]. Available from: https://seer.cancer.gov/statistics-network/explorer/

The Leukemia & Lymphoma Society. (2023). Blood cancer statistics. Retrieved from https://www.lls.org/facts-and-statistics/facts-and-statistics-overview

Xu, H., Ma, Z., Mo, X., Chen, X., Xu, F., Wu, F., Chen, H., Zhou, G., Xia, H., & Zhang, C. (2022). Inducing Synergistic DNA Damage by TRIP13 and PARP1 Inhibitors Provides a Potential Treatment for Hepatocellular Carcinoma. *Journal of Cancer, 13*(7), 2226-2237. https://doi.org/10.7150/jca.66020

Xu, Y., et al. (2020). Overexpression of TRIP13 in epithelial ovarian cancer is associated with poor clinical outcomes and promotes tumor growth by regulating the DNA damage response. *Cancer Medicine, 9*(8), 2864-2874. https://doi.org/10.1002/cam4.2948

Zhang, G., Zhu, Q., Fu, G., et al. (2019). TRIP13 promotes the cell proliferation, migration and invasion of glioblastoma through the FBXW7/c-MYC axis. *British Journal of Cancer, 121*(12), 1069-1078. https://doi.org/10.1038/s41416-019-0633-0